

THE SCHWERDTFEGER LIBRARY  
1225 W. Dayton Street  
Madison, WI 53706

VISSR ATMOSPHERIC SOUNDER

Monthly Progress Report No. 10  
For the Period 1 June 1974 to 30 June 1974

Contract No. NAS5-21965

For National Aeronautics and Space Administration  
Goddard Space Flight Center  
Glen Dale Road  
Greenbelt, Maryland 20771

By

V. E. Suomi, Principal Investigator  
L. A. Sromovsky, Co-Investigator

The University of Wisconsin  
Space Science and Engineering Center  
1225 West Dayton Street  
Madison, Wisconsin 53706

## TABLE OF CONTENTS

### INTRODUCTION

1. Rigorous Calibration of a Linear Radiometer	1
2. Characterization of the VAS and VAS Calibration Measurements	2
3. Calibration of the VAS Without the Auxiliary Space View	5
4. Calibration of the VAS Using the Auxiliary Space View	14
5. Computer Simulation of Alternative Techniques for VAS Calibration	17

## INTRODUCTION

Analysis of the simulator results is still in process. A report on diffractive misregistration will appear in next month's report. A revised calibration analysis has been completed and a few copies of the results have already been communicated to NASA. The full report of this work is enclosed.

Recently, renewed interest has been generated in using an auxiliary space view to improve the calibration accuracy of the VISSR Atmospheric Sounder (VAS). The analysis which follows details the quantitative improvements which can be expected from this proposed change. The present VAS calibration and the calibration using the auxiliary space view are discussed on the same footing, and compared in terms of errors produced under similar conditions of laboratory measurement errors and in-orbit degradations of optical components. The auxiliary space view appears to provide a significant improvement in reducing bias errors in the calibration, although whether the improvement is worth the cost of implementation is strongly dependent on what kind and amount of in-orbit degradation of the VAS is probable.

## 1. Rigorous Calibration of a Linear Radiometer

A linear radiometer (e.g. the VAS) produces an output signal linearly related to the radiation input. If  $N_T$  is the input radiance and  $V$  is the output voltage then they must satisfy the following equation

$$V = R N_T + V_o \quad (1-1)$$

where  $R$  is the responsivity of the radiometer and  $V_o$  is the system offset voltage. If  $R$  and  $V_o$  are known then the input radiance  $N_T$  is determined from the output  $V$  by the relation

$$N_T = (V - V_o) / R. \quad (1-2)$$

Calibration consists of determining  $V_o$  and  $R$  so that (1-2) can be applied. Since there are only two unknowns in equations (1-1) and (1-2) a rigorous determination can be made by exposing the radiometer to two different external radiation targets of known radiance magnitude and measuring the radiometer responses. This leads to a system of two linear equations

$$\begin{aligned} V_1 &= R N_1 + V_o \\ V_2 &= R N_2 + V_o \end{aligned} \quad (1-3)$$

which has the solution

$$\begin{aligned} R &= (V_2 - V_1) / (N_2 - N_1) \\ V_o &= (N_2 V_1 - N_1 V_2) / (N_2 - N_1). \end{aligned} \quad (1-4)$$

If the results of (1-4) are inserted into equation (1-2) we find the result

$$N_T = [(N_2 - N_1) V - (N_2 V_1 - N_1 V_2)] / (V_2 - V_1). \quad (1-5)$$

For the special case  $N_1 = 0$ , i.e., the radiometer uses empty space as one of the external calibration targets, we find

$$R = (V_2 - V_1) / N_2,$$

$$V_o \neq V_1, \text{ and} \quad (1-6)$$

$$N_T \neq N_2 (V - V_1) / (V_2 - V_1). \quad (1-7)$$

Equations (1-6) and (1-7) apply to the VAS with the exception that there is no real external radiance source  $N_2$  which can be used for calibration. Instead an internal blackbody is used for calibration, in which case an effective value for  $N_2$  must be determined. In the case of the VAS this effective value is the radiance of an external source which would produce the same voltage output which is produced by the internal calibration blackbody. The estimate for the effective value of  $N_2$  is based on optical constants of the VAS and temperature measurements of the optical components. The accuracy of the calibration is thus limited by the accuracy of the constants and temperatures used to estimate  $N_2$ .

## 2. Characterization of the VAS and VAS Calibration Measurements

A simplified description of the VAS and its radiation sources and targets is presented in Figure 1. This description includes the capability to view space bypassing the VAS telescope, although the case in which this option is not available will also be considered. There are four distinct measurements which must generally be considered in the VAS calibration.

These are defined below.

<u>VIEW</u>	<u>SIGNAL OUTPUT</u>	
space through the VAS telescope	$V_1 = \alpha (1 - \gamma) B (T_A) + V_o$	(2-1)

internal blackbody	$V_2 = \alpha B (T_s) + V_o$	(2-2)
-----------------------	------------------------------	-------

space bypassing the VAS telescope	$V_3 = \alpha \epsilon_m B (T_m) + V_o$	(2-3)
--------------------------------------	---	-------

external target	$V_4 = \alpha (\gamma N_T + (1 - \gamma) B (T_A)) + V_o$	(2-4)
--------------------	--	-------

The parameters used in expressions for the signal output are defined as follows:

$\alpha$  = responsivity of the VAS detector system  
(volts/unit radiance).

$\gamma$  = transmission of the VAS telescope.

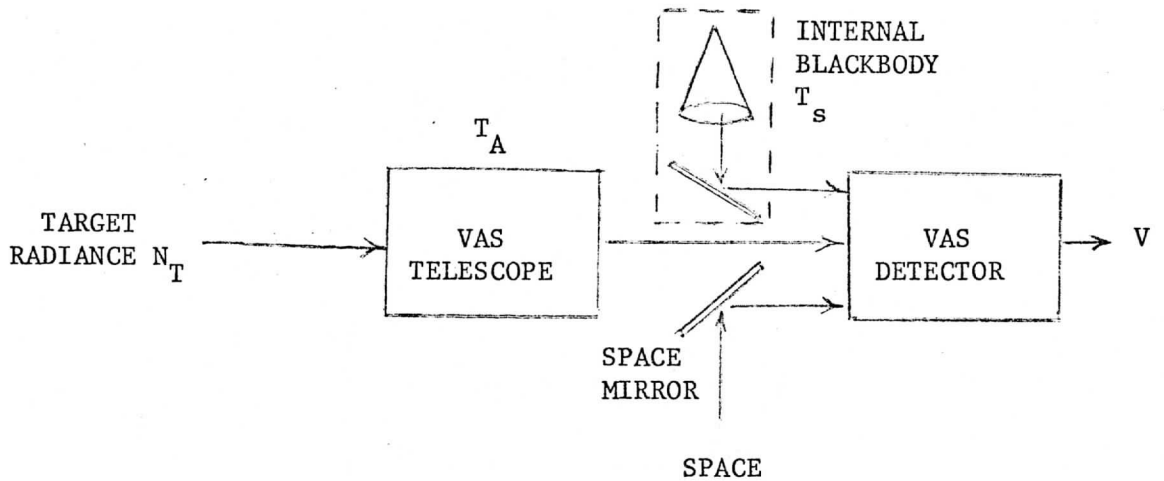
$T_A$  = weighted average temperature of the VAS  
telescope.

$T_s$  = temperature of the internal calibration  
blackbody.

$T_m, \epsilon_m$  = temperature and emissivity of the mirror  
used to reflect the auxiliary space view.

$B(T)$  = the plank radiance of a blackbody at  
temperature  $T$ .

The weighting used to obtain the average temperature  $T_A$  will be described later; the requirement it must satisfy is that  $T_A$  be chosen so that  $(1 - \gamma) B(T_A)$  is exactly the radiance contribution produced by the VAS telescope.



TARGET	=	Space, earth, or equivalent external blackbody.
VAS TELESCOPE	=	Scan mirror, primary telescope, and field lens.
VAS DETECTOR	=	Relay optics (excluding field lens), detectors, and electronics. Final output is a voltage signal V.
INTERNAL BLACKBODY	=	Blackbody cone and gold mirror at ambient temperature.
SPACE MIRROR	=	Mirror introduced into optical path to provide a space view which bypasses the VAS telescope.

FIGURE I. LUMPED DESCRIPTION OF THE VAS



### 3. Calibration of the VAS Without the Auxiliary Space View

#### 3.1 Basic Equations

In this case equation (2-3) for  $V_3$  does not apply. The equation corresponding to equation (1-7) relating a voltage output to radiance of an external target is just

$$N_T = (V_4 - V_1) / (\alpha \gamma) \quad (3-1)$$

where  $\alpha \gamma$  cannot be determined from the remaining measurements.

However, by estimating  $\gamma$  and  $T_A$   $\alpha$  can be determined by the equation

$$\alpha = (V_2 - V_1) [B(T_s) - (1 - \gamma) B(T_A)]^{-1}. \quad (3-2)$$

Inserting (3-2) into (3-1) we obtain the result

$$N_T = B(T^*) (V_4 - V_1) / (V_2 - V_1) \quad (3-3)$$

where  $B(T^*)$  is the effective value of the external blackbody radiance which produces the same response as the internal blackbody radiance  $B(T_s)$ . This is just the effective value of  $N_2$  of equation (1-7).  $B(T^*)$  is defined by the relation

$$B(T^*) = \frac{1}{\gamma} [B(T_s) - (1 - \gamma) B(T_A)]. \quad (3-4)$$

This same result could have been obtained by equating equations (2-4) and (2-2) with  $B(T^*)$  substituted for  $N_T$ .

The weighted average temperature  $T_A$  is determined by the relation

$$(1 - \gamma) B(T_A) = \sum_{i=1}^5 a_i B(T_i) \quad (3-5)$$

where the  $T_i$  and  $C_i$  values are defined in the following table in

which  $R_i$ ,  $\epsilon_i$  ( $=1 - R_i$ ),  $i = 1, 3$  are the reflectivities and emissivities

respectively of the three telescope mirrors,  $K$  is the central obscuration fraction, and  $\tau_f$  and  $\epsilon_f (=1 - \tau_f)$  are the reflectivity and transmission of the field lens.

<u>i</u>	<u>Component</u>	<u>Temperature</u>	<u><math>a_i</math></u>
1	scan mirror	$T_1$	$\epsilon_1 R_2 R_3 \tau_f (1-K)$
2	primary mirror	$T_2$	$\epsilon_2 R_3 \tau_f (1-K)$
3	secondary mirror	$T_3$	$\epsilon_3 \tau_f$
4	central obscuration	$T_4$	$K \tau_f R_3$
5	field lens	$T_5$	$\epsilon_f$

Note that the  $a_i$  satisfy the condition

$$\sum_{i=1}^5 a_i = 1 - \gamma, \text{ where} \quad (3-6)$$

$$\gamma = R_1 R_2 R_3 \tau_f (1-K). \quad (3-7)$$

Inserting (3-5) into (3-4) yields the expression

$$B(T^*) = \frac{1}{\gamma} [B(T_s) - \sum_{i=1}^5 a_i B(T_i)]. \quad (3-8)$$

Since all of the defined temperatures will normally be within a few degrees of  $T_s$  it is justifiable to make use of the Taylor expansion

$$B(T) = B(T_s) + \frac{\partial B(T_s)}{\partial T_s} (T - T_s) + \dots \quad (3-9)$$

to simplify equations (3-5) and (3-8) to the following forms

$$T_A = T_s + \frac{1}{(1-\gamma)} \sum_{i=1}^5 a_i (T_i - T_s), \quad (3-10)$$

$$T^* = T_s - \frac{1}{\gamma} \sum_{i=1}^5 a_i (T_i - T_s) \quad (3-11)$$

In previous analyses a set of optical constants  $C_i$  were used instead of the  $a_i$ . The relation between them is just a normalization

factor  $\gamma$ , i.e.

$$C_i = a_i/\gamma. \quad (3-12)$$

The sum is then constrained to satisfy

$$\sum C_i = \frac{1}{\gamma} - 1, \quad (3-13)$$

and equation (3-11) takes the form

$$T^* = T_s - \sum_{i=1}^5 C_i (T_i - T_s). \quad (3-14)$$

Expressions and nominal values for the  $C_i$  coefficients are listed below

$$\begin{aligned} C_1 &= \epsilon_1/R_1 &= 0.0417 \\ C_2 &= \epsilon_2/R_1 R_2 &= 0.0434 \\ C_3 &= \epsilon_3/R_1 R_2 R_3 (1-K) &= 0.0538 \\ C_4 &= K/(R_1 R_2 (1-K)) &= 0.2067 \\ C_5 &= \epsilon_f/(R_1 R_2 R_3 \tau_f (1-K)) &= 0.1495 \end{aligned} \quad (3-15)$$

where the fundamental constants were assumed to have the nominal values

$$\begin{aligned} R_1 &= R_2 = R_3 = 0.96 \\ \epsilon_1 &= \epsilon_2 = \epsilon_3 = 0.04 \\ K &= 0.16 \\ \tau_f &= 0.90 \\ \epsilon_f &= 0.10. \end{aligned} \quad (3-16)$$

The value of  $\gamma$  derived from these parameters is

$$\gamma = 0.6689. \quad (3-17)$$

A thermal analysis of the VISSR indicates that, except for eclipse conditions, values for worst case temperature gradients between the internal blackbody and the telescope components are as follows (day 172 results)

$$\begin{aligned}
 T_1 - T_s &= -3.34^\circ\text{K} \\
 T_2 - T_s &= -2.16^\circ\text{K} \\
 T_3 - T_s &= -8.54^\circ\text{K} \\
 T_4 - T_s &= -6.47^\circ\text{K} \\
 T_5 - T_s &= -2.16^\circ\text{K} \text{ (estimated as } 1/3 \text{ of } T_4 - T_s)
 \end{aligned}
 \quad \left. \vphantom{\begin{aligned} T_1 - T_s \\ T_2 - T_s \\ T_3 - T_s \\ T_4 - T_s \\ T_5 - T_s \end{aligned}} \right\} (3-18)$$

For day 172 gradients and the coefficients given in (3-15) the computed difference between  $T^*$  and  $T_s$  is just

$$T^* - T_s = 2.35^\circ\text{K}. \quad (3-19)$$

### 3.2 Effects of Errors

Errors in the VAS calibration result from two distinct sources: uncertainties in values of the fundamental optical constants ( $R_1, R_2$ , etc.), and errors in measurements of blackbody and telescope temperatures. Present estimates for these errors are presented in the following tables.

Table 3.2-1

#### VAS Temperature Errors

Thermistor, absolute calibration uncertainty	0.1°K
Telemetry uncertainty	0.08°K RMS
Temperature differences between sensor and other points on the measured component	probably negligible with the possible exceptions of the central obscuration and the field lens

Table 3.2-2

VAS Optical Constant Errors

Absolute errors in laboratory measurements	0.01
Systematic errors in laboratory measurements	0.005 (except for K)
Launch and in-orbit degradation	?

Although, once the VAS is operating in orbit, the main effect of these errors is to produce a bias error in  $T^*$ , it is useful to consider them as random errors temporarily so that the probability distribution of possible bias errors can be estimated.

It is advantageous for this error estimate to use equations (3-13) and (3-12) to reduce (3-14) to the form.

$$T^* = \frac{1}{\gamma} \left[ T_s - \sum_{i=1}^5 a_i T_i \right]. \quad (3-20)$$

Since all the  $a_i$ 's must satisfy equation (3-6), regardless of the values of  $R_1$ ,  $R_2$ ,  $R_3$ ,  $\tau$ , or  $K$ , they are not independent parameters and cannot be used as such to estimate variances in  $T^*$ . The effects of correlated errors in the  $a_i$ 's (and  $C_i$ 's as well) can be avoided by expressing the variance of  $T^*$  in terms of the independent parameters  $R_1$ ,  $R_2$ ,  $R_3$ ,  $K$ , and  $\tau$ . In terms of these parameters the variance of  $T^*$  is just

$$\begin{aligned} \sigma_{T^*}^2 = & \sum_{i=1}^3 \left( \frac{\partial T^*}{\partial R_i} \right)^2 \sigma_{R_i}^2 + \left( \frac{\partial T^*}{\partial \tau} \right)^2 \sigma_{\tau}^2 + \left( \frac{\partial T^*}{\partial K} \right)^2 \sigma_K^2 \\ & + \frac{1}{\gamma^2} \sigma_{T_s}^2 + \frac{1}{\gamma^2} \sum_{i=1}^5 a_i^2 \sigma_{T_i}^2 \end{aligned} \quad (3-21)$$

where the derivatives of  $T^*$  have the general form

$$\frac{\partial T^*}{\partial x} = \frac{1}{\gamma} \left\{ -T^* \frac{\partial \gamma}{\partial x} - \sum_{i=1}^5 T_i \frac{\partial a_i}{\partial x} \right\}, \quad (3-22)$$

where  $x$  denotes one of the independent optical parameters. The component derivatives are tabulated in Table 3.2-3. From these derivatives it is possible to evaluate (3-22) for each choice of  $x$ . Results of these evaluations are found in equations (3-23) through (3-27).

Table 3.2-3 Derivatives of Correlated Optical Parameters with Respect to Independent Parameters

$x$	$R_1$	$R_2$	$R_3$	$\tau$	$K$
$\frac{\partial \gamma}{\partial x}$	$\frac{\gamma}{R_1}$	$\frac{\gamma}{R_2}$	$\frac{\gamma}{R_3}$	$\frac{\gamma}{\tau}$	$\frac{-\gamma}{1-K}$
$\frac{\partial a_1}{\partial x}$	$\frac{-\gamma}{R_1}$	$\frac{a_1}{R_2}$	$\frac{a_1}{R_3}$	$\frac{a_1}{\tau}$	$\frac{-a_1}{1-K}$
$\frac{\partial a_2}{\partial x}$	0	$\frac{-a_2}{1-R_2}$	$\frac{a_2}{R_3}$	$\frac{a_2}{\tau}$	$\frac{-a_2}{1-K}$
$\frac{\partial a_3}{\partial x}$	0	0	$\frac{-a_3}{1-R_3}$	$\frac{a_3}{\tau}$	0
$\frac{\partial a_4}{\partial x}$	0	0	$\frac{a_4}{R_3}$	$\frac{a_4}{\tau}$	$\frac{a_4}{K}$
$\frac{\partial a_5}{\partial x}$	0	0	0	-1	0

$$\frac{\partial T^*}{\partial R_1} = \frac{-1}{\partial R_1} [T^* - T_1] \quad (3-23)$$

$$\frac{\partial T^*}{\partial R_2} = \frac{-1}{R_1 R_2} [R_1 (T^* - T_1) + (T_1 - T_2)] \quad (3-24)$$

$$\frac{T^*}{R_3} = \frac{-\tau}{\gamma} [(1-K) R_2 \{R_1 (T^* - T_1) + (T_1 - T_2)\} + (T_2 - T_3) + K(T_4 - T_2)] \quad (3-25)$$

$$\frac{\partial T^*}{\partial \tau} = \frac{-1}{\gamma} [R_2 R_3 (1-K) \{ R_1 (T^* - T_1) + (T_1 - T_2) \} + R_3 (T_2 - T_3) + K(T_4 - T_2) + (T_3 - T_5)] \quad (3-26)$$

$$\frac{\partial T^*}{\partial K} = \frac{R_3 \tau}{\gamma} [R_1 R_2 (T^* - T_1) + R_2 (T_1 - T_2) + (T_2 - T_4)] \quad (3-27)$$

Approximate forms for the above derivatives can be obtained by making the approximation

$$R_1 = R_2 = R_3 \approx 1. \quad (3-28)$$

In this approximation we obtain

$$\frac{\partial T^*}{\partial R_1} \approx \frac{(T_1 - T^*)}{R^4 \tau (1-K)}, \quad (3-29)$$

$$\frac{\partial T^*}{\partial R_2} \approx \frac{1}{R^2} (T_2 - T^*), \quad (3-30)$$

$$\frac{\partial T^*}{\partial R_3} \approx \frac{1}{R^3(1-K)} [(T_3 - T^*) - K (T_4 - T^*)], \quad (3-31)$$

$$\frac{\partial T^*}{\partial \tau} = \frac{1}{R^3(1-K)\tau} [(T_s - T^*) - K (T_4 - T^*)], \text{ and} \quad (3-32)$$

$$\frac{\partial T^*}{\partial K} = \frac{1}{R^2(1-K)} [T_4 - T^*]. \quad (3-33)$$

For day 172 temperature gradients we recall from equation (3-19) that

$$T^* = T_s + 2.35^\circ\text{K}, \quad (3-34)$$

which implies that

$$T_i - T^* = (T_i - T_s) - 2.35^\circ\text{K} \quad (3-35)$$

where  $T_i - T_s$  values are given in (3-18). For this specific case numerical values of (3-29) through (3-33) are tabulated along with temperature derivatives in Table 3.2-4.

Table 3.2-4 Numerical Values of  $\frac{\partial T^*}{\partial x}$  for Day 172 Temperature Gradients

<u>x</u>	<u><math>\frac{\partial T^*}{\partial x}</math></u>
R <sub>1</sub>	- 8.81°K
R <sub>2</sub>	- 4.89°K
R <sub>3</sub>	-13.25°K
τ	- 5.18°K
K	+11.40°K
T <sub>s</sub>	1.495
T <sub>1</sub>	- .0417
T <sub>2</sub>	- .0434
T <sub>3</sub>	- .0538
T <sub>4</sub>	- .2067
T <sub>5</sub>	- .1495

If we choose

$$\left. \begin{array}{l} \sigma_{R_i} \approx \sigma_{\tau} \approx \sigma_K \equiv \sigma_R \\ \sigma_{T_s} \approx \sigma_{T_i} \equiv \sigma_T \end{array} \right\} \quad (3-36)$$

then, for values listed in Table 3.2-4, equation (3-22) reduces to the result

$$\sigma_{T^*}^2 = 434^\circ\text{K}^2 \sigma_R^2 + 2.30 \sigma_T^2. \quad (3-37)$$

For expected uncertainties of

$$\sigma_R \approx .01, \quad \sigma_T = (.1^2 + .08^2)^{\frac{1}{2}} = .13^\circ\text{K} \quad (3-38)$$

we obtain the standard deviation of possible T\* bias errors of

$$\sigma_{T^*} = 0.29^\circ\text{K}. \quad (3-39)$$

Systematic errors and in-orbit degradation induced errors can also be treated using the derivatives of Table 3.2-4. In this case the



bias error in  $T^*$  is given by

$$\delta T^* = \sum_{j=1}^{11} \frac{\partial T^*}{\partial x_j} \delta x_j \quad (3-40)$$

where  $x_j$  ranges over all the optical and temperature parameters and  $\delta x_j$  is the systematic error of the  $x_j$ th parameter. For the assumed conditions.

$$\left. \begin{aligned} \delta T_s = \delta T_i = 0, \\ \delta K = 0, \text{ and} \\ \delta R_1 = \delta R_2 = \delta R_3 = \delta \tau \equiv \delta R, \end{aligned} \right\} \quad (3-41)$$

equation (3-40) takes the following form for day 172 temperature gradients:

$$\delta T^* = (-32.13^\circ\text{K}) \delta R. \quad (3-42)$$

Specific cases of interest are found in Table 3.2-5.

Table 3.2-5 Effects of Systematic Errors in Optical Constants on  $T^*$  for Day 172 Temperature Gradients

<u><math>\delta R</math></u>	<u><math>\delta T^*</math></u>
$\pm 0.005$ (systematic error in laboratory measurements)	$\mp 0.16^\circ\text{K}$
$-0.03$ (possible in-orbit degradation)	$+0.96^\circ\text{K}$

#### 4. Calibration of the VAS Using the Auxiliary Space View

##### 4.1 Basic Equations

As in the previous case the equation corresponding to equation (1-7) relating a voltage output to an external target radiance is just

$$N_T = (V_4 - V_1) / (\alpha \gamma), \quad (4-1)$$

which is derived from equations (2-1) and (2-4), and is identical to equation (3-1). As before, the parameter product  $\alpha\gamma$  cannot generally be determined from the remaining measurements without estimation of optical constants and temperature measurements. There is a difference in the present case in that it provides one additional measurement, i.e. equation (2-3), and requires estimation of two additional parameters, i.e.  $\epsilon_m$  and  $T_m$ .

At this point there are two approaches one can take in deriving the final calibration. The distinction between them arises from different choices of known and unknown parameters. The two approaches and their corresponding solutions are summarized below.

	<u>APPROACH NO. 1</u>	<u>APPROACH NO. 2</u>
"Known" parameters (must be directly measured or estimated)	$T_s, T_m, \epsilon_m, \gamma$	$T_s, T_m, \epsilon_m, T_A$
"Unknown" parameters (are derived from calibration measurements)	$T_A, \alpha$	$\gamma, \alpha$

Solution for  $\alpha$  (same for both approaches)

$$\alpha = (V_2 - V_3) / (B(T_s) - \epsilon_m B(T_m)) \quad (4-2)$$

Solution for  $T_A$  (Approach No. 1)

$$B(T_A) = (1 - \gamma)^{-1} [B(T_s) - \left(\frac{V_2 - V_1}{V_2 - V_3}\right) (B(T_s) - \epsilon_m B(T_m))] \quad (4-3)$$

Solution for  $\gamma$  (Approach No. 2)

$$\gamma = 1 - \frac{B(T_S)}{B(T_A)} + \frac{(v_2 - v_1)}{(v_2 - v_3)} \cdot \frac{B(T_S) - \epsilon_m B(T_m)}{B(T_A)} \quad (4-4)$$

Solution for  $T^*$ 

Approach No. 1

$$B(T^*) = \frac{1}{\gamma} \frac{(v_2 - v_1)}{(v_2 - v_3)} [B(T_S) - \epsilon_m B(T_m)] \quad (4-5)$$

Approach No. 2

$$B(T^*) = B(T_A) [B(T_S) - \epsilon_m B(T_m)] / [B(T_S) - \epsilon_m B(T_m) + \frac{v_2 - v_3}{v_2 - v_1} (B(T_A) - B(T_S))] \quad (4-6)$$

Even a cursory examination of equation (4-5) indicates that approach No. 1 is unsatisfactory; a quite probable 2.2% RMS error in  $\gamma$  ( $\sigma_\gamma^2 / \gamma^2 \approx 5 \sigma_R^2 / R^2$ ) leads directly to an unacceptable 2.2% RMS error in  $B(T^*)$  which is equivalent to an RMS error in  $T^*$  that ranges from 1.94°K for  $\nu = 680 \text{ cm}^{-1}$  to 0.5°K for  $\nu = 2700 \text{ cm}^{-1}$ . The effect of systematic errors is even worse. The reason this approach is so unsatisfactory is that it ignores telescope temperatures and does not make use of the fact that an isothermal VAS is perfectly calibrated by the internal blackbody. Thus it is not practical to calibrate the VAS without using a radiative model for the telescope itself. Only the second approach, which does make use of measured telescope temperatures, will receive any further discussion.

#### 4.2 Effects of Errors

Errors in the estimation of  $T^*$  by means of equation (4-6) can be determined by the same procedures used previously, i.e. the

the systematic bias error is found from the relation

$$\delta T^* = \left( \frac{\partial B(T^*)}{\partial T^*} \right)^{-1} \sum_{j=1}^{16} \frac{\partial B(T^*)}{\partial x_j} \delta x_j \quad (4-7)$$

and the bias error due to randomly distributed uncertainties (or the noise due to random errors) is found using the relation

$$\sigma_{T^*} = \left[ \left( \frac{\partial B(T^*)}{\partial T^*} \right)^2 \sum_{j=1}^{16} \left[ \frac{\partial B(T^*)}{\partial x_j} \right]^2 \sigma_{x_j}^2 \right]^{\frac{1}{2}} \quad (4-8)$$

where  $x_j$  ranges over all the optical and temperature parameters required for evaluation of equation (4-6) and where (4-6) is used to obtain the required derivatives of  $B(T^*)$ .

However, implementation of this approach using linearization of the Planck function and appropriate approximations is by no means straightforward. The complexity of equation (4-6) and the large number of independent parameters involved makes the derivation of meaningful analytic expressions tedious and obscure. As a result errors in the VAS calibration with the auxiliary space view are treated numerically by computer calculation.

A description of the computer calculation and comparative results for calibrations with and without the auxiliary space view are presented in Section 5.

## 5. Computer Simulation of Alternative Techniques for VAS Calibration

### 5.1 Basic Computational Procedure

The computational procedure can be summarized by the following steps:

- (1) Read in exact values of parameters which specify the state of the VAS instrument.
- (2) Calculate the exact value of  $T^*$  using exact values of all required parameters and without expanding the Planck function (this result is, of course, independent of calibration technique).
- (3) Read in bias errors and/or standard deviations for choosing random errors for each parameter which is measured or must be estimated to calculate  $T^*$  in orbit.
- (4) Calculate perturbed values for all parameters required to calculate  $T^*$  in orbit.
- (5) Using errored parameters calculate two values of  $T^*$  using in one case the  $T^*$  equation for the present VAS calibration and in the second case the  $T^*$  equation for the auxiliary space view calibration.
- (6) Determine the difference between the results of (5) and the results of (2) for each approach. This yields the  $T^*$  errors produced by the input parameter uncertainties.
- (7) For cases in which random errors are inserted steps (4) through (6) are repeated many times and RMS and mean results of (6) are obtained as a final output.

It should be noted that the general approach just discussed allows much greater flexibility than is needed in the initial error

analysis. Our basic approach initially is to determine partial derivatives of  $T^*$  with respect to all parameters involved in calculating it so that quick linear estimates of various kinds of errors can be estimated for the worst case day 172 temperature gradient situation.

## 5.2 Alternative Equations for $T^*$

The two methods for determination of  $T^*$  are: (1) the present VAS calibration discussed in section 3; and (2) the VAS calibration using an auxiliary space view, as discussed in section 4. The two methods have distinctly different expressions for estimating  $T^*$  and, unless all parameters are known exactly, these expressions yield different values for  $T^*$ . Denoting  $T_1^*$  as the  $T^*$  estimate for the present VAS calibration and  $T_2^*$  the result for the auxiliary space view approach, we may state the two determining equations as follows:

PRESENT VAS (METHOD 1)

$$B(T_1^*) = \frac{1}{\gamma} \left[ B(T_s) - \sum_{i=1}^5 a_i B(T_i) \right] \quad (5-1)$$

VAS WITH AUXILIARY SPACE VIEW (METHOD 2)

$$B(T_2^*) = \frac{[B(T_s) - \epsilon_m B(T_m)] \frac{1}{1-\gamma} \sum_{i=1}^5 a_i B(T_i)}{B(T_s) - \epsilon_m B(T_m) + \frac{V_2 - V_3}{V_2 - V_1} \left[ \frac{1}{1-\gamma} \sum_{i=1}^5 a_i B(T_i) - B(T_s) \right]} \quad (5-2)$$

The function  $B(T)$  stands for the Planck function

$$B_v(T) = C_1 v^3 \left[ \exp(C_2 v/T) - 1 \right]^{-1}$$

which, of course, depends on wavenumber  $\nu$  as well as  $T$ . The wavenumber dependence is implicit in equations (5-1) and (5-2). In both methods linearization of the Planck function is avoided, and  $T_1^*$  and  $T_2^*$  are determined from  $B(T_1^*)$  and  $B(T_2^*)$  using the inverse Planck function

$$T_i^* = C_2 \nu \left\{ \ln \left[ 1 + \frac{C_1 \nu^3}{B(T_i^*)} \right] \right\}^{-1}, \quad i = 1, 2. \quad (5-4)$$

All parameters used in equations (5-1) and (5-2) are defined in sections 2, 3 and 4. Note that when exact values of all parameters are employed we have the result  $T_1^* = T_2^* = T^*$ .

### 5.3 Numerical comparison of Partial Derivatives

For day 172 temperature gradients numerical values of partial derivatives were obtained from computer calculation by perturbing each parameter value separately and dividing the resultant  $T^*$  perturbation by the magnitude of the input perturbation, i.e.

$$\frac{\partial T_i^*}{\partial x_j} \approx \frac{T_i^*(x_1, x_2, \dots, x_j + \delta x_j, \dots) - T_i^*}{\delta x_j}, \quad i = 1, 2. \quad (5-5)$$

The eleven derivatives relevant to Method 1 and the sixteen relevant to Method 2 are listed in Table 5-1. The values for  $\frac{\partial T_1^*}{\partial x}$  in Table 5-1 are found to be in substantial agreement with the values of  $\frac{\partial T^*}{\partial x}$  in Table 3.2-4, although the latter, which are based on linearization of the Planck function and on approximation of derivative expressions, do show some small differences with the present results which is to be expected.

The interesting comparison is between derivatives for Method 1

and derivatives for Method 2. Although the derivatives with respect to temperature are in close agreement, the derivatives with respect to optical constants are quite different. On the average derivatives of  $T_1^*$  are larger in magnitude than those of  $T_2^*$ . In addition, all the  $T_1^*$  derivatives imply additive bias errors resulting from in-orbit degradation, while the  $T_2^*$  derivatives allow for considerable cancellation of degradation induced errors (since  $\epsilon_m$  increases as a result of degradation of the space view mirror the sign of  $\partial T_2^*/\partial \epsilon_m$  implies some cancellation with changes due to degradation of  $R_1$ ,  $R_2$  and  $\tau$ . This effect will be quantitatively treated in the next section.

With regard to the temperature derivatives both methods show an overwhelming dependence on  $T_s$ , a moderate dependence on  $T_4$  and  $T_5$  and a fairly weak dependence on  $T_1$ ,  $T_2$ , and  $T_3$ . Note that the dependence of  $T_2^*$  on  $T_m$  is exceptionally weak, a fortunate result considering the probable difficulty in measuring  $T_m$  accurately.

#### 5.4 Absolute and Comparative Error Estimates

The effect of randomly distributed parameter uncertainties on  $T^*$  errors can be calculated from the derivatives listed in Table 5-1 and the usual relation

$$\sigma_{T^*}^2 = \sum_j \left( \frac{\partial T^*}{\partial x_j} \right)^2 \sigma_{x_j}^2 \quad (5-6)$$

where  $x_j$  denotes one of the independent parameters and  $\sigma_{x_j}$  its uncertainty. Individual parameter uncertainties have been estimated previously for all parameters except those new ones required by Method 2, i.e.  $\epsilon_m$ ,  $T_m$ ,  $V_1$ ,  $V_2$ , and  $V_3$ . The first of these,  $\epsilon_m$ , will



Table 5-1 Numerical Comparisons of T\* derivatives for Alternative Calibration Methods

<u>x</u>	$\left(\frac{\partial T_1^*}{\partial x}\right)$	$\left(\frac{\partial T_2^*}{\partial x}\right)$
	<u>PRESENT VAS</u>	<u>VAS WITH AUXILIARY SPACE VIEW</u>
R <sub>1</sub>	-5.74 K	+1.56°K
R <sub>2</sub>	-4.50 K	+2.94°K
R <sub>3</sub>	-11.79 K	-5.19°K
τ	-3.49 K	+4.62°K
K	+10.70 K	+2.48°K
ε <sub>m</sub>	-	+7.69°K
T <sub>s</sub>	+1.478	+1.514
T <sub>1</sub>	-.041	-.044
T <sub>2</sub>	-.042	-.046
T <sub>3</sub>	-.051	-.055
T <sub>4</sub>	-.198	-.214
T <sub>5</sub>	-.146	-.158
T <sub>m</sub>	-	+0.004
V <sub>1</sub>	-	+0.0049°K/mv
V <sub>2</sub>	-	-0.0014°K/mv
V <sub>3</sub>	-	-0.0035°K/mv

NOTE: Voltage derivatives assume a worst case gain yielding 50% of 4.75V for the internal blackbody measurement. Also note that digitized level spacing is approximately 18 mv.

be treated as the other optical parameters  $R_1, R_2$ , etc.  $T_m$  is more difficult to measure than any other temperature. However, even a  $1^\circ\text{K}$  error in  $T_m$  has such a small effect that it is reasonable to ignore its contribution to the  $T^*$  variance altogether. The voltage measurements are assumed to be average results of sufficiently many measurements to reduce the voltage noise to at least the level of the 8 bit quantization noise (which has the approximate RMS value of 5 mv). Under these conditions voltage variances also have a negligible effect on  $\sigma_{T^*}$ .

For an assumed measurement uncertainty of  $\sigma_R$  in the optical parameters  $R_1, R_2, R_3, \tau, K$ , and  $\epsilon_m$ , and  $\sigma_T$  in  $T_s$  and  $T_i, i = 1, 5$  the uncertainty in estimating  $T^*$  obtained from Table 5-1 and equation 5-6 is found to satisfy the following relationships for Methods 1 and 2:

$$\sigma_{T_1^*} = [\sigma_R^2 \times (319^\circ\text{K}^2) + 2.25 \sigma_T^2]^{1/2} \quad (5-7)$$

$$\sigma_{T_2^*} = [\sigma_R^2 (125^\circ\text{K}^2) + 2.37 \sigma_T^2]^{1/2} \quad (5-8)$$

It should be remembered that these relationships are specific to the temperature gradients predicted for Day 172. For expected errors listed in Tables 3.2-1 and 3.2-2 it is appropriate to use

$$\sigma_R = .01, \sigma_T = 0.13^\circ\text{K} \quad (5-9)$$

in equations (5-7) and (5-8) to determine best estimates for the standard deviation of possible  $T^*$  errors. The results are

$$\sigma_{T_1^*} = 0.26^\circ\text{K}, \text{ and} \quad (5-10)$$

$$\sigma_{T_2^*} = 0.23^\circ\text{K}. \quad (5-11)$$

Thus we see that both methods have substantially the same performance under the assumed conditions of randomly distributed errors, although

it should be noted that  $\sigma_{T_2}^*$  has significantly less dependence on  $\sigma_R^2$  than does  $\sigma_{T_1}^*$ .

When systematic errors are considered the two methods diverge considerably in their sensitivity to errors in optical component parameters. The effects of systematic errors  $\delta x_j$  in the optical parameters  $x_j$  on the systematic error in  $T^*$  (denoted by  $\delta T^*$ ) are estimated using Table 5-1 derivatives and the relation

$$\delta T^* = \sum_j \frac{\partial T^*}{\partial x_j} \delta x_j. \quad (5-12)$$

First let us consider the case of uniform systematic error, i.e.

$$\delta R_1 = \delta R_2 = \delta R_3 = \delta \tau = (-\delta \epsilon_m) \equiv \delta R. \quad (5-13)$$

The systematic error in  $K$  is assumed to be zero. In this case, again for day 172 gradients we find

$$\delta T_1^* = (-25.5^\circ\text{K}) \delta R, \quad (5-14)$$

$$\delta T_2^* = (-3.8^\circ\text{K}) \delta R. \quad (5-15)$$

Table 5-2 Comparative Estimates of  $T^*$  Bias Errors Resulting from Uniform Systematic Optical Constant Errors

$\delta R$	$\delta_{T_1}^*$ (PRESENT VAS)	$\delta_{T_2}^*$ (VAS WITH AUXILIARY SPACE VIEW)
$\pm 0.005$ (systematic error in laboratory measurements)	$\mp 0.13^\circ\text{K}$	$\mp 0.02^\circ\text{K}$
$-0.03$ (possible in-orbit degradation of optical components)	$+0.77^\circ\text{K}$	$\pm 0.11^\circ\text{K}$

For uniform systematic errors Method 2 is seen to have a very strong advantage over Method 1 (bias errors are reduced by a factor of 7).

For the case of nonuniform systematic errors results vary considerably with the distribution of errors among the optical components. Let us assume a fixed transmission loss of 20%, i.e.  $\gamma$  changes from 0.6689 to

an in-orbit value of 0.5351, and then calculate the values of  $\delta T_1^*$  and  $\delta T_2^*$  as a function of how the transmission loss is distributed among the optical components for some limited cases of interest. Results are presented in Table 5-3. For simplicity, when more than one optical component is assumed to degrade, all are assumed to degrade equally.

Table 5-3. T\* Bias Errors for a 20% Transmission Loss as a Function of which Elements are Degraded

PARAMETERS WHICH ARE DEGRADED EQUALLY TO YIELD A COMBINED 20% TRANSMISSION LOSS	INDIVIDUAL PARAMETER CHANGE	$\delta T_1^*$	$\delta T_2^*$	
$R_1$ (scan mirror)	-0.192	+1.10°K	-0.30°K	
$R_1, R_2$	-0.101	+1.04°K	-0.46°K	
$R_1, R_3$	-0.101	+1.78°K	+0.37°K	
$R_1, R_2, R_3$	-0.069	+1.52°K	+0.05°K	
$\tau$ (field lens)	-0.180	+0.63°K	-0.83°K	
$R_1, R_3, \tau$	-0.068	+1.43°K	-0.07°K	
$R_1, R_2, R_3, \tau$	-0.052	+1.33°K	-0.20°K	
$\epsilon_m$ also degraded by same amount as other parameters (increased).	$R_1$	-0.192	-	+1.18°K
	$R_1, R_3$	-0.101	-	+1.15°K
	$R_1, R_2, R_3$	-0.069	-	+0.58°K
	$\tau$	-0.180	-	+0.55°K
	$R_1, R_3, \tau$	-0.068	-	+0.45°K
	$R_1, R_2, R_3, \tau$	-0.052	-	+0.20°K

In all cases considered in Table 5-3, except for all degradation residing in the field lens,  $\delta T_2^*$  is smaller, and often very much smaller, than  $\delta T_1^*$  if  $\epsilon_m$  is not allowed to degrade significantly.

If  $\epsilon_m$  is also degraded by the same magnitude as those parameters which produce the transmission loss the results are not quite so dramatic. In the latter case, although  $\delta T_2^*$  is significantly smaller on the average, there are two cases for which  $\delta T_1^*$  is smaller than  $\delta T_2^*$ . Of course, a meaningful comparison of the two methods would be greatly aided by some knowledge of the relative probabilities of these cases or perhaps others which have not been considered.

Another approach to estimating in-orbit degradation effects is to define a fixed degradation per element and examine  $T^*$  errors as different combinations of elements are allowed to degrade. Results for a fixed degradation of 0.05 are presented in Table 5-4.

If the conditions considered in Table 5-4 are reasonable, then Method 2 would again appear to have a strong advantage over Method 1. As before, this conclusion is conditional on the probability of each of the situations considered.

If we assume, for lack of any specific degradation probability information, that all uses considered in both tables are equally likely (a truly gross assumption), then it is possible to summarize the relative errors probable for the two methods by finding average and absolute average values for the total sample set. Results of this calculation, presented in Table 5-5, also point up the advantages of Method 2.

Table 5-4. T\* Bias Errors Resulting from 0.05 Degradation per Element as a Function of the Combination of Elements which Degrade

<u>PARAMETERS WHICH DEGRADE</u>	<u><math>\delta T_1^*</math></u>	<u><math>\delta T_2^*</math></u>	<u>NET TRANSMISSION LOSS</u>
$R_1$	+0.29°K	-0.08°K	5.2%
$R_1, R_2$	+0.51°K	-0.23°K	10.1%
$R_1, R_3$	+0.88°K	+0.18°K	10.1%
$R_1, R_2, R_3$	+1.10°K	+0.03°K	14.8%
$\tau$	+0.17°K	-0.23°K	5.6%
$R_1, R_3, \tau$	+1.05°K	-0.05°K	15.1%
$R_1, R_2, R_3, \tau$	+1.28°K	-0.20°K	19.6%
$R_1, \epsilon_m$	-	+0.30°K	5.2%
$R_1, R_2, \epsilon_m$	-	+0.15°K	10.1%
$R_1, R_3, \epsilon_m$	-	+0.56°K	10.1%
$R_1, R_2, R_3, \epsilon_m$	-	+0.41°K	14.8%
$\tau, \epsilon_m$	-	+0.15°K	5.6%
$R_1, R_3, \tau, \epsilon_m$	-	+0.33°K	15.1%
$R_1, R_2, R_3, \tau, \epsilon_m$	-	+0.18°K	19.6%

Table 5-5. Average Results for all Degradation Cases Considered in Tables 5-3 and 5-4.

	<u>METHOD 1 (PRESENT VAS)</u>	<u>METHOD 2 (USING AUXILIARY SPACE VIEW)</u>
Bias error averaged over all cases	+1.01°K	+0.04°K
Bias error absolute value averaged over all cases	1.01°K	0.35°K
% cases exceeding 1 K absolute error	64%	4%
% cases exceeding 0.5 K absolute error	86%	22%